Photo-induced phenomena in GeO_2 glass

Nobuaki Terakado, Keiji Tanaka*

Department of Applied Physics, Graduate School of Engineering, Hokkaido University, Sapporo 060-8629, Japan

Abstract

Photo-induced changes in GeO_2 glass have been studied in optical and structural properties. Band-gap excitation gives rise to modifications in mid-gap optical absorption and photo-luminescence spectrum. It also produces electron-spin signals at $g \simeq 1.995$ and 2.008. Raman-scattering spectrum becomes sharper, x-ray diffraction patterns show disappearance of a crystalline peak, and illuminated surfaces expand. These observations can be accounted for by assuming bond transformations from rutile-like to defective quartz-like structures and/or from small to large rings. These photo-induced changes in GeO_2 are comparatively discussed with those in SiO_2 and GeS_2.

PACS: 61.82Ms, 61.43.Fs, 71.55Jv, 78.20.Ci

Keywords: Photoinduced Effect P210; Germania G140

*corresponding author; keiji@eng.hokudai.ac.jp

1. Introduction

It has been known that a variety of photo-induced phenomena appear in group VIb glasses [1,2]. For instance, Bragg reflectors are inscribed in Ge-doped SiO_2 fibers using excimer lasers [3], holographic images are stored in sulfide films [4], and optical phase-changes in telluride films have now been commercialized [5]. Nevertheless, fundamental mechanisms and unified understanding of these phenomena remain to be arduous problems in solid state science.

Under such circumstances, studies on the photo-induced phenomenon in GeO_2 appear to be valuable, at least, in three respects. First, the result can provide related insights into formation processes of photo-induced Bragg-reflectors in Ge-doped SiO_2, in which Ge atoms seem to play important roles [3]. Second, pure GeO_2 optical fibers and waveguides are promising to some applications [6,7], so that photo-induced changes should be explored. The last, which may be the most interesting from fundamental viewpoints, is that the result on GeO_2 can bridge photo-induced behaviors in the oxide glass such as SiO_2 and the chalcogenide such as GeS_2. Photo-induced phenomena in the oxide and the chalcogenide have similar and dissimilar features [1,2], and accordingly, studies from a unified point-of-view will be valuable.

Following these motivations, the present authors have recently investigated photo-induced phenomena in sputtered GeO_2 films [8]. It is shown that the change depends upon pressure of ambient air, which provides H_2O into the film under illumination. The feature seems be governed by a defective and inhomogeneous non-crystalline structure, which is similar to that in evaporated GeS_2 films [9].

Here, we extend the study to melt-quenched GeO_2 glass. Such studies are needed because the glass property depends upon preparation methods. Actually, qualitatively different photo-induced changes between film and bulk have sometimes been reported. For instance, the previous work on sputtered GeO_2 films demonstrates a photo-induced refractive-index decrease [8], while GeO_2 bulk glass is known to provide a photo-induced refractive-index increase [10]. Such an opposite behavior also appears in GeS_2; i.e., as-evaporated GeS_2 films undergo photo-bleaching, while bulk GeS_2 provides photo-darkening [9]. Notable differences have been pointed out also for SiO_2 [3,11]. We will see in the present study that GeO_2 glass exhibits unique photo-induced changes, which are different from those in the sputtered films and also in SiO_2 and GeS_2 bulk glasses.

2. Experiments

Samples employed were GeO_2 bulk glasses, which were prepared with due caution. This

is because thin flakes are needed for investigating photo-induced phenomena upon band-gap illumination [1,9] and, as is known, the glass is likely to crystallize [12]. Accordingly, before every measurement, a small (~0.1 g) ingot was prepared (the total being ~20 times) and shaped into an appropriate thickness, and most measurements were done within one week. Owing to the limited preparation procedures, the present samples appeared frosty a little, probably reflecting inclusion of small voids. But, experimental results were not governed by the voids, as described in 3.

Sub-gram ingots were prepared from crystalline GeO_2 powders with a purity of 5-nine (Furu-uchi Chem. Co., GEC-33206A). The powders were placed on a flat Pt plate, heated in a furnace at 1400 °C for 2 h in ambient atmosphere, and then, taken outside from the furnace for air-quenching. The ingot was polished, as in a previous study [9], to a discs with lateral dimension of 2 - 5 mm and thickness of 25 - 300 μm [13]. Then, the disc was annealed in ambient atmosphere for 10 h at 500 °C, which was slightly lower than the glass-transition temperature T_g of ~580 °C [12].

The samples, which had optical band-gap energy E_g of ~ 5.8 eV [12,14,15], were exposed to three kinds of excitations having different photon energies. Sub-gap excitations ($\hbar\omega < E_g$) with photon energies of 3.5 eV and 4.6 eV were obtained from third- and fourth-harmonic generators attached to a Nd:YAG laser (Continuum, Surelite I), which emitted light pulses with duration of 5 ns and repetition of 5 Hz. Band-gap excitation of 6.4 eV ($\hbar\omega < E_g$) was obtained from an ArF excimer laser (Tuilaser, S-200), which emitted light pulses with duration of 10 ns and repetition of 20 Hz. Power densities of these excitations with 3.5, 4.6, and 6.4 eV were adjusted, respectively, to 500, 100, and 20 mJ/cm^2/pulse, all of which provided an absorbed dose of ~10^5 J/cm^3 at 10^4 pulses, which corresponded to an absorbed photon number of ~10^{23} cm^{-3} [16]. Super-gap (core-electron) excitation was obtained from a ^{60}Co source as γ-rays, which have characteristic photon energies of 1.17 and 1.33 MeV and a typical intensity of 0.1 MGy/day. These excitations were supplied to GeO_2 samples at room temperature in ambient atmosphere. In addition, the laser light (3.5, 4.6, and 6.4 eV) was supplied also in vacuum of 10^{-2} Pa at room temperature and 80 K, in which the sample was fixed in an optical cell having a synthetic SiO_2 window. In some cases, illuminated samples were annealed at 500 °C for 3 h in order to examine thermal reversibility of photo-induced changes.

Exposure effects were investigated in several macroscopic and microscopic properties. Optical transmittance was measured at wavelengths of 210 – 1200 nm ($\hbar\omega$ = 5 - 1.0 eV). In a short wavelength region of 210 – 350 nm (3.5 – 5.9 eV), we used a single-beam spectrometer consisting of a Xe lamp, a monochromator, a sample box, and a photo-multiplier, in which

separation between a sample and the photo-multiplier surface was reduced to ~5 cm. This equipment was effective in obtaining transmission spectra, which were less influenced by light scattering, because it could detect transmitted and partially-scattered light. At longer wavelengths of 340 - 1200 nm (1.0 - 3.5 eV), absorption spectra were monitored using photo-thermal deflection spectroscopy, which is known to be less sensitive to light scattering, the experimental detail being reported previously [17]. Photo-luminescence (PL) spectra in a range of 1.5 - 4.0 eV were obtained at 80 K, in order to increase PL signals, using light sources of the ArF excimer laser (6.4 eV, 5 mJ/cm^2/pulse, and 20 Hz) and the Nd:YAG-laser fourth-harmonic (4.6 eV, 10 mJ/cm^2/pulse, and 5 Hz), a single polychromator (Jobin-Yvon, CP-140-103), and a linear photo-diode array (Hamamatsu, S5933-1024S). Obtained spectra were normalized with respect to a black body radiation at 3300 K. Photo-induced changes in sample thickness were measured using a profile monitor (TAYLOR-HOBSON, Talystep). Raman-scattering spectra were taken using an Ar-ion laser (488 nm), a He-Cd laser (442 nm), a triple polychromator (Jobin-Yvon, T64000), and a cooled charge-coupled-device. Spectral measuring time was typically 15 min, which did not provide noticeable photo-induced effects. X-band electron-spin resonance (ESR) measurements were carried out at 80 K using a Bruker spectrometer (EMX) with a measuring time of 3 min and a microwave power of 0.02 mW. Spin density was calibrated using a $CuSO_4(5H_2O)$ standard. X-ray diffraction patterns were obtained using a rotating Cu target (Rigaku, RU-300) and a graphite monochromator. Differential radial distribution functions (RDFs) were calculated as in the previous [8]. Infra-red transmission spectra were measured using a Fourier-transform spectrometer (Perkin Elmer, 1650).

3. Results

Fig. 1(a) shows optical absorption spectra in as-quenched (solid circles) and annealed (open circles) GeO_2 glasses. Light scattering could still affect these spectra, and accordingly, the vertical axis may be read as attenuation. However, as illustrated, the present spectrum is roughly consistent with those obtained for sputtered films [8,18,19] and bulk glasses [12,14,15,20,21]. The optical gap, which can be defined at the photon energy with an absorption coefficient of 10^3 cm^{-1}, is located at around ~5.8 eV. Below the absorption edge, both the present and the previous spectra for bulk glasses possess an absorption shoulder at 4 - 5 eV, which has been ascribed to oxygen-deficient defects such as Ge homo-polar bonds (≡Ge–Ge≡) [20,22,23], two-fold coordinated Ge (–Ge–) [22], and Ge E' centers (≡Ge·) [20,24]. In addition, the present samples show a broad absorption at ~2 eV, which can be ascribed to nano-crystalline Ge [25,26].

Two kinds of annealing effects have been detected. One is an appreciable absorption (attenuation) increase at ~2 eV, as shown in Fig. 1(a), which may be due to a change in light scattering and/or an increase in nano-crystalline Ge [25,26]. The other annealing effect, which is more clearly seen in a difference spectrum plotted in a linear scale, Fig. 1(b), is an absorption decrease at ~5 eV, which is consistent with those reported previously [12]. This decrease seems to be resolved into small and large changes at around 4.2 eV and 5.0 V, which may be ascribed, respectively, to Ge E' centers [20,24] and to the oxygen-deficient centers [12,20,22], which include Ge homopolar bonds and two-fold coordinated Ge. These absorption decreases at ~5 eV suggest that the annealing at 1 atm reduces the density of these oxygen-deficient defects, which implies that the annealing yields more stoichiometric glass structures. Therefore, we focus hereafter mostly upon photo-induced effects in annealed samples.

Fig. 1(c) shows photo-induced changes in absorption spectra in the annealed GeO_2. Since excitation doses could not be adjusted accurately and the samples were different in thickness, only rough features should be emphasized, in which the most notable is the increase in optical absorption at 4 - 6 eV. It should be mentioned that the 3.5, 4.6, and 6.4 eV excitations in vacuum at 300 and 80 K have given quantitatively similar absorption changes to those shown here. In detail, the sub-gap excitations of 3.5 and 4.6 eV induce nearly the same absorption increase at around 4.5 - 5.0 eV. Such an absorption increase may be related through a Kramers-Kronig relation with a photo-induced increase in refractive-index of $\sim 10^{-5}$ evaluated at $\hbar\omega = 3.5$ eV [10]. On the other hand, the (super-)gap excitations of 6.4 eV and ~1 MeV seem to be effective in increasing absorption bands at 4.2 and ~5.0 eV. The steep attenuation increase at the absorption edge (~5.5 eV) by γ-ray excitation, which is consistent with a previous report [20], implies radiation-induced light scattering. It should be mentioned here that the absorption increase by 4.6 eV pulses in Fig. 1(c) has been mostly recovered with a heat treatment at 500 °C for 3 h. That is, produced defects can be annealed.

Fig. 1(d) shows PL spectra obtained using weak 6.4 eV pulses in a spectral range of 1.5 - 4.0 eV in annealed and illuminated GeO_2. We see in the annealed sample (solid line) a broad PL peak at ~2.1 eV, the position being similar to the low-energy absorption in Fig. 1(a). With excitation of 6.4 eV and 10^5 J/cm^3 at room temperature, this 2.1 eV peak seems to be converted to a 2.6 eV peak, as shown by the dashed line and more clearly by the dotted difference spectrum. On the other hand (not shown), when PL is measured using sub-gap light of 4.6 eV, only the 2.1 eV peak appears, which decreases with the 6.4 eV band-gap excitation, which may be regarded as a kind of PL fatigue [1]. These results obtained by using 4.6 eV and 6.4 eV suggest that the 2.1 eV and 2.6 eV components have different PL origins.

However, it is difficult to identify the origins. Previous studies suggest, at least, three possibilities for several PL peaks appearing at 1.8 - 2.3 eV, which are non-bridging oxygen hole center (≡Ge–O·) [27], self-trapped exciton [28], and nano-crystalline Ge [26,29-32]. Accordingly, it is difficult to identify an origin of the 2.1 eV PL. On the other hand, for the 2.6 eV PL peak, Qiu et al. have suggested that it can arise from two-fold coordinated Ge [33], which also causes an absorption shoulder at ~5 eV [22]. A similar suggestion was made previously by Skuja [34], although related energies were slightly different. We note that the Qius' model is consistent with the present observation in a respect that both the 5 eV absorption and the 2.6 eV PL increase with light excitation. This model also appears to be consistent with the fact that the 2.6 eV PL cannot be produced by 4.6 eV light (< 5 eV).

As shown in Fig. 2, the band-gap excitation of 6.4 eV has produced ESR signals. In these spectra, an intense sharp signal has appeared at $g \simeq 2.001$ (dashed part), which is a spurious arising from an irradiated cryostat window, the origin probably being Si E' centers [24], and accordingly, it should be neglected. Without that, the annealed sample gives only a weak signal at 2.008. After excitation with 6.4 eV pulses of 10^5 J/cm^3 at room temperature, the 2.008 signal grows and a signal at $g \simeq 1.995$ appears, the both increasing to densities of ~10^{17} cm^{-3}. These changes resemble those observed in GeO_2 upon exposure to γ -ray irradiation [12,20,24]. Origins of these signals at 1.995 and 2.008 are assumed, respectively, to be Ge E' centers and oxygen excess centers, which include non-bridging oxygen hole centers (≡Ge–O·) and peroxy radicals (≡Ge–O–O·) [20,24].

In short, the optical and ESR results suggest the photo-induced enhancement of several kinds of oxygen-deficient and oxygen-excess defects. Here, the optical measurements can detect the oxygen-deficient defects due to their high optical cross-sections [34], and the ESR spectroscopy detects only the defects having un-paired electrons.

Fig. 3 shows photo-induced surface deformations induced by 4.6 (squares) and 6.4 eV (circles) excitations as a function of doses [36]. The vertical scale presents a fractional thickness change $\Delta d / \alpha^{-1}$, which is obtained through normalization of real changes Δd in surface height by penetration depths α^{-1} (calculated from the absorption coefficient) of excitation light. Absolute expansion is, e.g., upon 10^4 pulses of 4.6 eV excitation (the penetration depth α^{-1} being ~50 μm), $\Delta d \simeq$100 nm, which corresponds to ~0.2 % when normalized. We see that, as a function of pulse number, the annealed sample *expands*, irrespective of excitation at 1 atm (solid symbols) and in vacuum (open symbols). We also see that expansion kinetics for 6.4 eV excitation changes at ~10^4 pulses (~10^5 J/cm^3). Above this threshold dose, the expansion occurs with surface roughening, which implies that the photo-induced change consists of, at least, two stages. Probably related with this feature is

that the expansion at ~10^4 pulses can be recovered by annealing for 3 h at 500 °C, while the annealing cannot recover the rough deformation induced by 10^5 pulses. It is interesting to mention here that the as-quenched GeO_2 has exhibited volume compaction, which is opposite to the expansion (Fig. 3) in the annealed samples.

It may be valuable to mention an interesting observation shown in the inset in Fig. 3. In the deformation experiment, we have used a metallic pin-hole plate with a thickness of 150 μm and a diameter of 120 μm, on to which a GeO_2 sample is attached and through which the sample is exposed to laser excitation. After the exposure, we obtain a circular fringe-type deformation on the GeO_2 sample, an example being shown in the inset. (Accordingly, the average expansion height is plotted in Fig. 3.) This fringe deformation resembles one appearing on the surface of As_2S_3 glass, which has been exposed to laser light through a pin hole [37]. The origin can be ascribed to spatially-varying volume changes induced by interference fringes, which are produced by direct incident light and reflected light at the inner wall of the pin hole.

Fig. 4 shows Raman-scattering spectra of GeO_2 and a photo-induced change. The overall spectral shape is consistent with previous results [12,38]. The most prominent 410 cm^{-1} peak is identified to a symmetric stretching mode of bridging oxygen (≡Ge-O-Ge≡), and the small 850 cm^{-1} hump is due to asymmetric stretching modes of the oxygen. The small peak at ~60 cm^{-1} is the so-called Boson peak, the origin remaining controversial [39]. Other features are not clear. For instance, Barrio et al. [40] and Giacomazzi et al. [38] theoretically suggest that planar 3-membered rings give some structure at around 500 - 530 cm^{-1}, which has not been resolved in the present measurement. It is also known that nano-crystalline Ge gives a Raman-scattering peak at 300 cm^{-1} [25] and the two crystalline forms (described in 4.1.) of GeO_2 produce peaks at 440 cm^{-1} and 700 cm^{-1} [41], but no related traces can be pointed out in the present spectra.

The Raman-scattering measurements have manifested two kinds of photo-induced changes. One is a small change for the Boson peak at ~60 cm^{-1}, which is more clearly seen when probed using 488 nm light and analyzed in HV configuration (not shown). That is, 10^4 pulses of 6.4 eV (and also 4.6 eV) excitation have reduced the Boson-peak intensity to 0.8 - 0.9 times of the original intensity, which recovers with annealing at 500 °C and 3 h. This change may correspond to a similar modification detected in GeO_2-SiO_2 glasses [42]. The other, which is shown in Fig.4, is a slight but appreciable shift accompanying narrowing of the 410 cm^{-1} main peak to a higher wave number by ~20 cm^{-1}, which is also reversible with the annealing.

Fig. 5 shows X-ray results. Overall shapes of X-ray diffraction patterns, in which three halos appear at $2\theta \simeq 22°$, 38°, and 64°, are consistent with previous results [12,43].

Differential RDFs have been calculated, and a typical result is shown in the upper inset, which is also consistent with the previous [12,43]. However, a closer look on the diffraction pattern can notice a small shoulder at $2\theta = 26^{\circ}$, which appears to be a crystalline peak when the halo component is subtracted, as shown in the lower inset. The peak has a full-width angle at half maximum of ~1°, suggesting a crystallite size of ~20 nm through the Sherrer's equation. However, it is difficult to identify a substance giving rise to this peak, because the position is roughly the same with those of the most intense peak arising from several candidates such as hexagonal GeO_2 (~26°), tetragonal GeO_2 (~29°), high-pressure phases of GeO_2 (~27° and ~28°), and crystalline Ge (~28°) [44].

As shown in the lower inset, 6.4eV band-gap excitation makes this crystalline peak smaller. This change implies that, under the excitation, the unidentified crystal merges into amorphous network. That is, the amorphous structure becomes more homogeneous with light excitation. In contrast, no photo-induced changes in the RDF have been detected, which means that no appreciable photo-induced changes occur in short-range structures.

Finally, results on infra-red transmission are mentioned. As in the previous study [8], we have measured transmission spectra and its photo-induced change at a wave number region of 400 - 4000 cm^{-1}. But, no photo-induced changes in vibrational modes of GeO_2, which are located at 400 - 1000 cm^{-1}, cannot be resolved. On the other hand, it has been found that, when exposed to excitations of 4.6 and 6.4 eV at 1 atm, the 3300 cm^{-1} modes arising from H_2O and -OH appear [45], which disappear with successive annealing. However, when the sample is exposed in vacuum, no such changes have been seen. These different results are contrastive to the irrelevance of atmosphere to the photo-induced changes described so far. Therefore, it is reasonable to assume that the hydrolytic reaction cannot be a major process governing the observed optical and structural changes shown in Figs. 1 - 5.

4. Discussion

4.1. Photo-induced change

Marked photo-induced changes observed in the annealed GeO_2 glass are the volume expansion (Fig. 3), the Boson-peak reduction and the shift of the main Raman peak (Fig. 4), the reduction of a crystalline x-ray peak (Fig. 5), and defect creation of several kinds (Figs. 1 and 2). However, it is difficult to draw a unique microscopic picture from these observations. In the following, therefore, we propose a tentative model, which can explain these observations in a coherent way.

It is known that there exist three common GeO_2 polymorphs, which are tetragonal (rutile-type), hexagonal (quartz-like), and glassy [12]. Unlike SiO_2, the stable GeO_2 crystal at

room temperature and 1 atm is the tetragonal, although the hexagonal GeO_2 can ordinary be retained as a meta-stable phase. In the tetragonal GeO_2, Ge is 6-fold coordinated, consisting of $GeO_{6/2}$ octahedral units, and in the hexagonal it is 4-fold coordinated with $GeO_{4/2}$ tetrahedral units. It has also been suggested that the GeO_2 glass contains the $GeO_{4/2}$ and $GeO_{6/2}$ units [12, 28, 46], which is consistent with the stability of the tetragonal and the hexagonal crystal in a similar degree [12]. In correspondence with these atomic structures, densities for the hexagonal, the tetragonal, and glassy GeO_2 are reported, respectively, to be 4.2, 6.2, and 3.7 g/cm^3 [47]. And, the optical band-gaps are known to be 5.6 [47], 4.7 [48], and ~5.8 eV [47], respectively. In addition, it is reasonable to assume that the GeO_2 glass has similar defective structures to those in SiO_2 glass [34]. Among those, the most notable may be small (3- and 4-membered) rings [40] and point-defect-like structures such as E' centers [24] and two-fold coordinated cations [22]

Taking these structural insights into account, we propose a model illustrated in Fig. 5. It presumes, as suggested previously [46], that the annealed GeO_2 glass contains a little amount of $GeO_{6/2}$ octahedral units and small rings. And, photo-excitation transforms these high-density elements, which may accompany some strains, to $GeO_{4/2}$ tetrahedral units and point defects such as Ge E' centers and two-fold coordinated Ge. The photo-excitation makes the heterogeneous structure more homogeneous and defective.

This model is consistent with the present observations as follows: The reduction in strain and high-density units can naturally provide a volume expansion, shown in Fig. 3. The strain reduction may also be responsible for the shift and narrowing of the Raman-scattering peak in Fig. 4. On the other hand, the reduction of $GeO_{6/2}$ octahedral units can be related with the intensity decrease of the crystalline X-ray peak. We here can estimate from the densities of the two crystals [47] and a typical volume expansion of ~1 % (Fig. 3) that the annealed sample contains $GeO_{6/2}$ bonding structures with a volume fraction of 0.5 - 1 %, provided that the high density unit is completely converted to hexagonal-like $GeO_{4/2}$ units. This small concentration may be consistent with the un-detection of a related Raman-scattering peak at 700 cm^{-1} of the tetragonal GeO_2 crystal [41]. The optical and ESR results shown in Figs. 1 and 2, which demonstrate photo-induced defect formation of some kinds, probably suggest that the reduction of the $GeO_{6/2}$ units and small rings accompanies creation of a lot (~10^{17} cm^{-3}) of defects. The thermal reversibility confirmed for the induced absorption (Fig. 1c), surface deformation (Fig. 3), and Raman-scattering spectrum (Fig. 4), is consistent with this model.

However, the above model is tentative. We, at present, have no convincing evidence of the $GeO_{6/2}$ octahedral units and small rings. More sensitive structural experiments are needed for further studies. In addition, identification of the absorption and PL peaks is

insufficient in comparison with that made for SiO_2 [34], partly because the spectra for GeO_2 are not sharp.

Finally, it may be valuable to note marked differences in photo-induced phenomena in GeO_2 glass and sputtered films. In the previous study [8], we have proposed that the photo-induced phenomena in the sputtered film can be understood by assuming a porous amorphous structure, into which H_2O diffuses under light excitation, which is responsible for a volume expansion. In the present bulk glass, however, we assume a heterogeneous amorphous structure, which becomes more homogeneous and defective upon light excitation. In short, the film undergoes the extrinsic chemical reaction, while the bulk seems to possess intrinsic structural changes.

4.2. Comparison

It is now possible to compare the photo-induced phenomena in SiO_2, GeO_2, and GeS_2 glasses. Table 1 summarizes some fundamental properties, marked photo-induced changes, and plausible mechanisms. Common to all these glasses is that the normal-bonding structure consists of the tetrahedral units of $Si(Ge)O(S)_{4/2}$. Nevertheless, in consistent with different bonding angles of Si(Ge)-O(S)-Si(Ge), the units in $Si(Ge)O_2$ are connected in a corner-shared way, while GeS_2 contains edge-shared connections [49], which can be regarded as 2-membered rings. On the other hand, $Si(Ge)O_2$ are believed to contain small rings such as 3- and 4-membered [11,40], and as noted above, GeO_2 may contain a little amount of $GeO_{6/2}$ units [46].

Photo-induced optical changes in the oxides and the chalcogenide are contrastive [1,2]. The most prominent change in $Si(Ge)O_2$ is the increase in mid-gap absorption [20,34,50], i.e. defective absorption, which is in marked contrast to the photo-darkening (red-shift of optical absorption edge) in chalcogenide glasses [1,2]. To the authors' knowledge, no photo-darkening has been reported for $Si(Ge)O_2$, and a result for As_2O_3 [51] has not been reproduced. The photo-induced mid-gap absorption and the photo-darkening can be ascribed, respectively, to three-dimensional rigid structure and the low-dimensional flexible structure [1, 2].

Photo-induced volume changes are more contrastive. SiO_2 exhibits the so-called radiation compaction [52], while GeS_2 undergoes the volume expansion [53], which is common to the most of covalent chalcogenide glasses [54,55]. Tanaka has proposed that the different volume changes in SiO_2 and GeS_2 can be interpreted using a relative glass density [54], which can be evaluated as a density ratio $R_\rho = \rho_g / \rho_c$ (< 1), where ρ_g and ρ_c are the glass density and the density of a corresponding crystal. In small R_ρ glasses such as SiO_2 ($R_\rho \simeq 0.83$), the structure is assumed to be open-spaced consisting of corner-shared $SiO_{4/2}$ units, in which

radiation compaction occurs upon electronic excitation. On the other hand, a dense glass with large R_ρ, which implies a compact glassy structure, tends to expand upon excitation through photo-induced structural disordering, which may be analogous to the Shottky-type defect formation in alkali-halide crystals. We here can envisage that an excitation produces a unique quasi-stable structure, which is energetically higher than thermally-relaxed (annealed) states.

The present work demonstrates that annealed GeO_2 also expands upon light excitation, in contrast to that in SiO_2. It is suggested that, in SiO_2, the volume compaction occurs with formation of small rings [11]. In contrast, in GeO_2, the volume expansion can be related with the reductions of $GeO_{6/2}$ units and small rings. Following the above notion, we can assume, taking $R_\rho \simeq 3.7/4.2 = 0.88$ (the densities being taken from [47], where ρ_c is of the hexagonal form) in GeO_2 into account, that the compaction-expansion boundary exists at $R_\rho \simeq 0.85$.

5. Conclusions

To obtain a unified insight into the photo-structural changes in oxide and chalcogenide glasses, we have investigated several features in GeO_2 glass. Photo-induced optical changes in GeO_2 are similar to those in SiO_2, while as for photo-induced volume changes GeO_2 exhibits an expansion in a similar way to that in GeS_2. The common optical change to $Si(Ge)O_2$ can be related with rigid three-dimensional network structures, while the volume expansion in GeO_2 is ascribable to a unique and dense glass structures.

Acknowledgements

The authors thank Professor H. Hosono and Dr. A. Saitoh for ESR measurements and Dr. T. Gotoh for photo-deflection spectroscopy measurements. The author (N. T.) also thanks financial supports from the 21st century Centre-of-Excellence program "Topological Science and Technology" by the Ministry of Education, Culture, Sports, Science and Technology of Japan.

References

[1] K. Shimakawa, A. Kolobov, S. R. Elliott, Adv. Phys. 44 (1995) 475.

[2] K. Tanaka, in: G. Lucovsky, M. Popescu (Eds.), Optoelectronic Materials and Devices, vol. 1, INOE Publishing House, Bucharest, 2004, pp. 43 - 64.

[3] G. Pacchioni, L. Skuja, D.L. Griscom (Eds.), Defects in SiO_2 and Related Dielectrics: Science and Technology, Kluwer Academic Publishers, Dordrecht, 2000.

[4] J.M. Gonzales-Leal, P. Krecmer, J. Prokop, S.R. Elliott, in: A.V. Kolobov (Ed.),

Photo-induced Metastability in Amorphous Semiconductors, Wiley-VCH, Weinheim, 2003, Chap. 20.

[5] T. Ohta, S.R. Ovshinsky, in: A.V. Kolobov (Ed.), Photo-induced Metastability in Amorphous Semiconductors, Wiley-VCH, Weinheim, 2003, Chap. 18.

[6] Z. Yin, P.E. Jessop, B.K. Garside, Appl. Opt. 22 (1983) 4088.

[7] S. Sakaguchi, S. Todoroki, Appl. Opt. 36 (1997) 6809.

[8] N. Terakado, K. Tanaka, J. Non-Cryst. Solids 351 (2005) 54.

[9] K. Tanaka, Y. Kasanuki, A. Odajima, Thin Solids Films 117 (1984) 251.

[10] Y. Watanabe, J. Nishii, H. Moriwaki, G. Furuhashi, H. Hosono, H. Kawazoe, J. Non-Cryst. Solids 239 (1998) 104.

[11] K. Awazu, J. Non-Cryst. Solids 337 (2004) 241.

[12] A. Margaryan, Germanate Glasses, Artech House, Boston, 1993.

[13] The sample thickness, 25 - 300 μ m, was varied so that light could penetrate into the sample. For sub-gap light of 3.5 and 4.6 eV, the thickness was adjusted to ~300 and ~50 μ m, which were comparable to the penetration depths of the laser light in to GeO_2. For band-gap light of 6.4 eV, the penetration depth was ~10 μ m. However, the present glass ingots were very fragile, and accordingly, 25 μ m-thick samples were inspected instead. In some cases, samples were exposed to light at both surfaces for enhancing exposure effects. For γ -rays, the penetration depth was estimated to be ~5 cm, and thick samples could be employed.

[14] A.J. Cohen, H.L. Smith, J. Phys. Chem. Solids 7 (1958) 301.

[15] J.M. Jackson, M.E.Wells, G. Kordas, D.L. Kinser, R.A. Weeks, R.H. Magruder Ⅲ, J. Appl. Phys. 58 (1985) 2309.

[16] For this calculation, absorption coefficients are taken from Fig. 1.

[17] K. Tanaka, T. Gotoh, N. Yoshida, S. Nonomura, J. Appl. Phys. 91 (2002) 125

[18] P. Bohac, L. Jastrabik, D. Chvostova, V. Zelezny, Vacuum 41 (1990) 1466.

[19] L. Pajasova, D. Chvostova, L. Jastrabik, J. Polach, J. Non-Cryst. Solids 182 (1995) 286.

[20] R.A. Weeks, T. Purcell, J. Chem. Phys. 43 (1965) 483.

[21] A.N. Trukhin, P. Kulis, J. Non-Cryst. Solids 188 (1995) 125.

[22] H. Hosono, Y. Abe, D.L. Kinser, R.A. Weeks, K. Muta, H. Kawazoe, Phys. Rev. B 46 (1992) 11445.

[23] T. Tamura, G.-H. Lu, R. Yamamoto, Phys. Rev. B 69 (2004) 195204.

[24] T.E. Tsai, D.L. Griscom, E.J. Friebele, J. Appl. Phys. 62 (1987) 2264.

[25] J.R. Heath, J.J. Shiang, A.P. Alivisatos, J. Chem. Phys. 101 (1994) 1607.

[26] S. Okamoto, Y. Kanemitsu, Phys. Rev B 54 (1996) 16421.

[27] L. Skuja, H. Hosono, M. Mizuguchi, B. Guttler, A. Silin, J. Lumines. 87 (2000) 699.
[28] A.N. Trukhin, J. Non-Cryst. Solids 189 (1995) 291.
[29] Y. Maeda, Phys. Rev. B 51 (1995) 1658.
[30] X.M. Wu, M.J. Lu, W.G. Yao, Surf. Coat. Tech. 161 (2002) 92.
[31] G. Kartopu, S.C. Bayliss, V.A. Karavanskii, R.J. Curry, R. Turan, A.V. Sapelkin, J. Lumines. 101 (2003) 275.
[32] A.N. Trukhin, J. Jansons, H.-J. Fitting, T. Barfels, B. Schmidt, J. Non-Cryst. Solids 331 (2003) 91.
[33] J. Qiu, N. Wada, F. Ogura, K. Kojima, K. Hirao, J. Phys.: Condens. Matter 14 (2002) 2561.
[34] L. Skuja, H. Hosono, M. Hirano, Proc. SPIE 155 (2001) 4347.
[35] Such kinetics was not inspected for the 4.6 eV sub-gap excitation due to the limited pulse-repetition rate of 5 Hz.
[36] Thickness changes by 3.5 eV light were not examined, and the change could not be evaluated for γ-ray, since a knife edge or a pin hole was needed for step measurements.
[37] H. Hisakuni, K. Tanaka, Opt. Lett. 20 (1995) 958.
[38] L. Giacomazzi, P. Umari, A. Pasquarello, Phys. Rev. Lett. 95 (2005) 75505.
[39] B.E. Hubbard, J.J. Tu, N.I. Agladze, A.J. Sievers, Phys. Rev. B 67 (2003) 144201.
[40] R.A. Barrio, F.L. Galeener, E. Martinez, R.J. Elliott, Phys. Rev. B 43 (1993) 15672.
[41] T.P. Mernagh, L.-G. Liu, Phys. Chem. Minerals 24 (1997) 7.
[42] F.X. Liu, J.Y. Qian, X.L. Wang, L. Liu, H. Ming, Phys. Rev. B 56 (1997) 3066.
[43] S. Kohara, K. Suzuya, J. Phys.: Condens. Matter, 17 (2005) S77.
[44] J. Haines, J.M. Leger, C. Chateau, Phys. Rev. B 61 (2000) 8701.
[45] The peak grows monotonically with light pulses, reaching to the absorbance of ~0.1 after 6.4 eV exposures of 5×10^4 pulses.
[46] Y.D. Yiannopoulos, C.P.E. Varsamis, E.I. Kamitsos, Chem. Phys. Lett. 359 (2002) 246.
[47] N.M. Ravindra, R.A. Weeks, D.L. Kinser, Phys. Rev. B 36 (1987) 6122.
[48] M. Stapelbroek, B.D. Evans Solid State Commun. 25 (1978) 959.
[49] S. Blaineau, P. Jund, D.A. Drabold, Phys. Rev B 351 (2003) 54.
[50] Y. Ikuta, K. Kajihara, M. Hirao, H. Hosono, Appl. Opt. 43 (2004) 2332.
[51] W.M. Pontuschka, P.C. Taylor, Solid State Commun. 38 (1981) 573.
[52] W. Primak, Phys. Rev. 110 (1957) 1240.
[53] H. Hamanaka, K. Tanaka, S. Iizima, Solid State Commun. 33 (1980) 355.
[54] K. Tanaka, Phys. Rev. B 57 (1998) 5163.
[55] K. Shimakawa, A. Ganjoo, J. Opt. Adv. Mater. 3 (2001) 167.

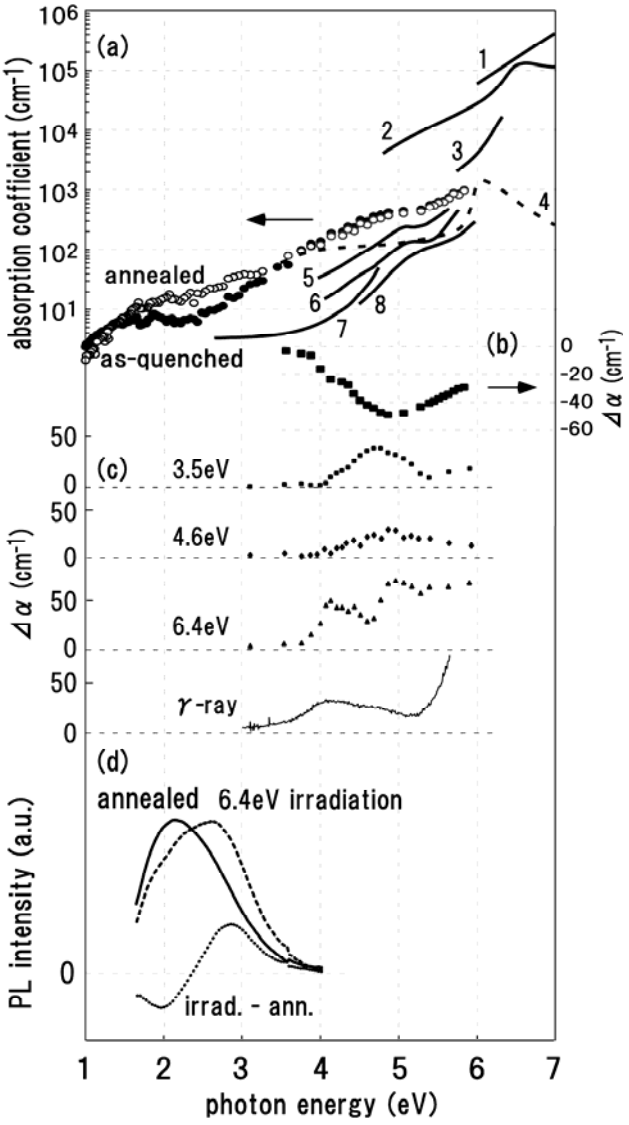

Fig. 1. (a) Optical absorption/attenuation spectra, (b) a change induced by annealing, (c) photo-induced absorption changes $\Delta\alpha$, and (d) photo-luminescence spectra of GeO_2 glass. In (a), solid and open circles present absorption spectra of as-quenched and annealed (500 °C for 10 h) GeO_2. Previous results on sputtered films (1 [19], 2 [8], 3 [18]) and bulk glasses (4 [12], 5 [14], 6 [15], 7 [20], 8 [21]) are also shown. (b) shows an annealing effect $\Delta\alpha$ at ~5 eV by solid squares with the linear right-hand side axis. (c) shows absorption increases induced by photo-excitation with photon energies written (3.5, 4.6 and 6.4 eV) and absorbed doses of ~10^5 J/cm^3 and by γ-ray with a dose of 1 MGy, which have been provided at room temperature in air. (d) shows PL spectra obtained at 80 K using weak 6.4 eV pulses in annealed (solid line) and illuminated (dashed line) GeO_2, and the photo-induced spectral change (dotted line).

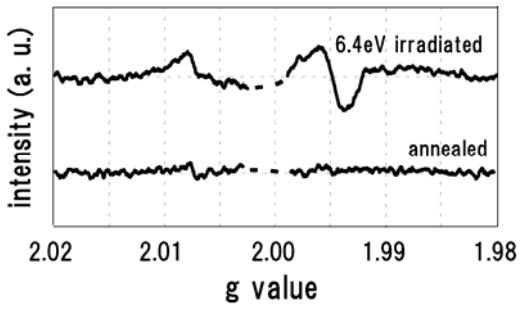

Fig. 2. ESR spectra of annealed (lower) and irradiated (upper) GeO_2.

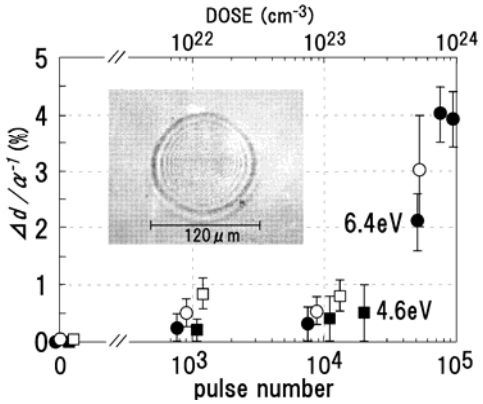

Fig. 3. Fractional changes $\triangle d/\alpha^{-1}$ in sample thickness induced by 4.6 eV (squares) and 6.4 eV (circles) pulses in vacuum (open symbols) and at 1 atm (solid symbols). $\triangle d$ is a real expansion height, and α is the absorption coefficient so that α^{-1} can be regarded as the penetration depth of excitation light. The inset photograph, which is taken using a Nomarski-type interference microscope, shows a surface of a GeO_2 sample which has been exposed to 10^4 pulses of 6.4 eV excitation through a pin hole with diameter of 120 μ m.

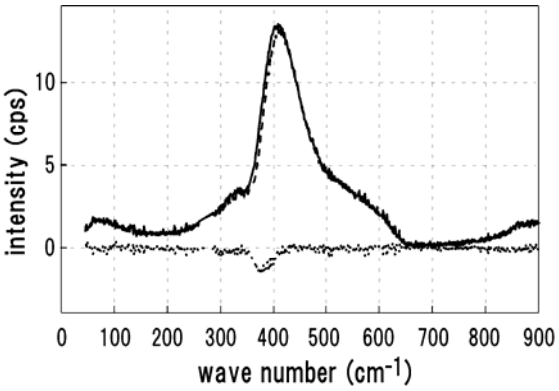

Fig. 4. Raman-scattering spectra (unpolarized) of GeO_2 before (solid line) and after (dashed line) an exposure to 10^4 pulses of 6.4 eV light. The spectra are probed using weak 442 nm light. The dotted line in the lower part shows a photo-induced change.

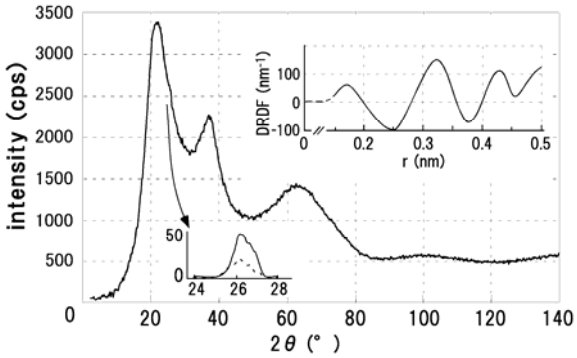

Fig. 5. X-ray diffraction pattern, differential radial distribution function (DRDF), and a photo-induced change at $2\theta \simeq 26^{o}$. The solid and dashed lines in the photo-induced change correspond to an annealed sample and its illuminated state after an exposure to 10^4 pulses of 6.4 eV excitation.

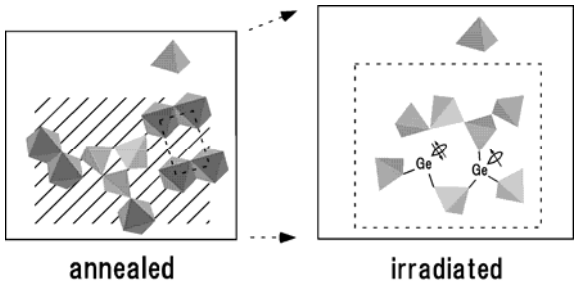

Fig. 6. Schematic illustrations of annealed and irradiated GeO_2, which accompanies a photo-induced volume expansion.

	SiO_2	GeO_2	GeS_2
cation-coordination number	4	4 (6?)	4
unit connection	corner-sharing	corner-sharing	corner and edge-sharing
E_g (eV)	~ 10	5.8	3.2
T_g (K)	1500	850	750
photo-induced optical change	mid-gap absorption	mid-gap absorption	photo-darkening
photo-induced volume change	compaction	expansion	expansion
R_ρ	0.83	0.88	0.92
mechanism	structural disordering	homogenization?	structural disordering

Table 1. Fundamental properties (upper) and photo-induced changes (lower) in the three glasses listed. R_ρ is a density ratio defined as ρ_g / ρ_c (< 1), where ρ_g and ρ_c are the glass density and the density of a corresponding crystal. Light excitation is presumed to be provided at room temperature.